DYNAMIC STIFFNESS ANALYSIS AND ISOLATION EFFECTIVENESS OF VIBRATION ISOLATION PLATFORM USING PNEUMATIC SPRING WITH AUXILIARY CHAMBER

Vo Ngoc Yen Phuong[1], Le Thanh Danh[2], Nguyen Minh ky[1]
[1]Ho Chi Minh City University of Technology and Education, Vietnam
[2] Ton Duc Thang University, Vietnam

Received 02/4/2019, Peer reviewed 27/5/2019, Accepted for publication 10/6/2019

ABSTRACT

This paper will introduce a vibration isolation platform using the pneumatic cylinder with an auxiliary chamber (shorted the platform with auxiliary chamber). Firstly, the pressure model of the air spring including the pneumatic cylinder with the auxiliary chamber is analyzed. Instead of experiment, the Amesim software is used as the virtual prototype technology to verify the analysis solution of this spring. The result of this verification confirms that the analysis solution shows close agreement with the virtual simulation. Secondly, the complex dynamic stiffness of the vibration isolation platform is determined. The effects of the volume of the auxiliary chamber on the dynamic stiffness of the isolation platform are analyzed. Finally, the isolation performance of the platform with and without the auxiliary chamber is compared. The analysis result shows that the platform with auxiliary chamber can offer a promising isolation performance. This presentation furnishes a clear understand of the dynamic stiffness of an air spring with auxiliary chamber as well as the application of the air spring for designing isolation models.

Keywords: *Pneumatic cylinder; Auxiliary chamber; Dynamic stiffness; Isolation platform; Virtual simulation.*

1. INTRODUCTION

As known, isolators are often used for protection of the machinery, equipment … as well as improvement of their life cycle. Nowadays, the development in different fields of engineering science, the machinery and equipment work very accurately. The equipment which has high accuracy, especially, instrumentation, is easily sensitive to external vibration, shock. Hence, isolators with variable stiffness [1-2] are preferable to ones with constant stiffness which often use the coil spring or rubber whose stiffness is constant [3-4]. One of the main issues of an isolator with constant stiffness is that it is too difficult to adjust the stiffness according to the change of the isolated load as well as enhance the isolation response meanwhile the isolator with variable stiffness can overcome this issue. For recent years, the magnetic springs [5-8] have been studied deeply for vibration isolation. Besides, with a variable in stiffness, these magnetic elastic elements can be simply controlled to upgrade the isolation effectiveness.

As an alternative, the isolation models using the air spring are used widely in engineering practice. M.W. Holtz et al. [9] analyzed theoretically and investigated experimentally a suspension seat using the air spring. The air spring force is controlled to improve the isolation performance of the seat suspension system as studied by I. Maciejewski et al. [10-12]. Besides, S. Oman et al. [13] presented successfully a model for estimating the fatigue life of the air spring. M.M. Moheyeldein et al. [14] investigated the dynamic response of the air spring suspensions, providing more comfortable and easy handling performances than the passive suspension. In addition, a position controller for the seat suspension using air spring

proposed and carried out–experimentally by C.M. Lee et al [15]. R.G. Todkar et al [16-17] developed an air damper and investigated the effects of the mass ratio and the air damper characteristic on the resonant response of an air vibration absorber, resulting in that an optimal value of the air damping ratio for minimizing the motion transmissibility of the system obtained.

The purpose of this work is an air spring with an auxiliary chamber is suggested and analyzed theoretically. To assess the actual performance and analysis solution of the pneumatic cylinder with auxiliary chamber, a virtual prototype technology via the Amesim software is employed. Then, an isolation platform using the above suggested air spring is presented. The effect of the volume of the auxiliary chamber on the dynamic stiffness of the platform is investigated.

2. Pneumatic spring model

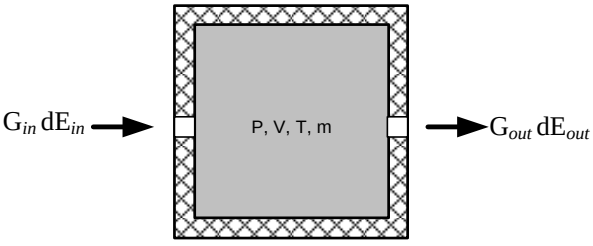

Fig.1 *Schematic diagram of pneumatic working chamber*

In general, consider the sketch of a pneumatic working chamber as in Fig. 1. Without the heart change, the thermodynamic equation in the air spring is described as following:

$$dE_{in} = dE_{ch} + dE_{ae} + dE_{out} \tag{1}$$

in which dE_{in} and dE_{oou} are the air energies of input and output lines, dE_{ch} is the air energy in spring, dE_{ae} is the work of air expansion. These energies are given as following:

$$\begin{aligned} dE_{in} &= C_p T_{in} G_{in} \\ dE_{out} &= C_p T G_{out} \\ dE_{ch} &= C_v m_{air} dT + C_v T dm_{air} \\ dE_{ae} &= PdV \end{aligned} \tag{2}$$

where C_p and C_v are specific heat capacities at constant pressure and volume, respectively. T_{in} is the temperature of air at the inlet; m_{air}, T and P are the mass, the temperature and pressure of the air in the air spring, V is the volume of the working chamber. G_{in} and G_{out} are mass low rates at inlet and outlet.

From the ideal air equation, we have:

$$\begin{aligned} PV &= m_{air} RT \\ m_{air} dT &= \frac{PdV + VdP - RTdm_{air}}{R} \end{aligned} \tag{3}$$

with R is the gas constant (R=287J/Kg.K)

Substituting Eq.(2-3) into Eq.(1), the air spring internal pressure equation is expressed as below:

$$\dot{P} = \frac{n}{V}\left(G_{in} RT_{in} - G_{out} RT - P\dot{V}\right) \tag{4}$$

where n=C_p/C_v is the ratio of specific heat capacity.

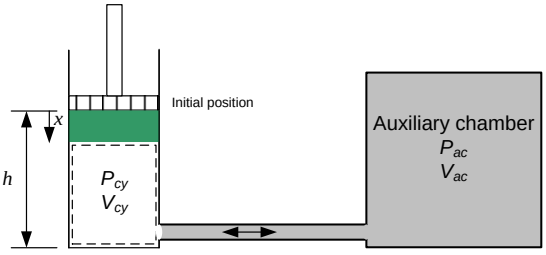

Fig.2 *Model of pneumatic cylinder with auxiliary chamber*

A model of the pneumatic cylinder with the auxiliary chamber is shown in Fig. 2. When the gas flows from the cylinder into the chamber, causing a displacement of the piston an announce x, by using Eq. (4), the pressure changing equations in the cylinder and the auxiliary chamber are expressed as following:

$$\dot{P}_{cy} = \frac{n}{V_{cy}}\left(-G_{out} RT - P\dot{V}_{cy}\right) \tag{5}$$

$$\dot{P}_{ac} = \frac{n}{V_{ac}} G_{in} RT \tag{6}$$

P_{cy} and P_{ac} are the pressure in the cylinder and the auxiliary chamber, respectively.

Ignoring the air leakage and the pressure drop in the line, we have:

$$G_{out} = G_{in}$$
$$P_{cy} = P_{ac} = P \quad (7)$$

Finally, the pressure change in the air spring with the auxiliary chamber is obtained as below:

$$\dot{P} = \frac{nP}{(h-x)A + V_{ac}} A\dot{x} \quad (8)$$

herein, A is the effectiveness area of the cylinder, h is the height of the cylinder as presented in Fig. 2.

By integrating from *0 to x*, the air pressure in the cylinder at an arbitrary position is expressed as following

$$P = P_o \left(\frac{Ah + V_{ac}}{Ah + V_{ac} - Ax} \right)^n \quad (9)$$

herein P_o is initial pressure of the air spring.

3. Virtual model of the pneumatic cylinder with auxiliary chamber

In order to verify the above analysis results, a virtual prototyping technology is used through Amesim software by which the virtual model of the cylinder with the auxiliary chamber is built as shown in Fig. 3. The result from the virtual model is compared with that obtained from analysis as plotted in Fig. 4. The effective area of the cylinder A=0.002m^2, the length of the piston stroke h=150mm, the initial pressure of the cylinder P_o is set at a value of 2.5 bar, the volume of the auxiliary chamber V_{ac} is set at the value of 0.001m^3, 0.01m^3, 0.015m^3 and 0.020m^3. It can be seen that the pressure obtained from the virtual model is always smaller than that given by Eq. (6) excepting the initial position. Because of the analysis solution neglects the dead volume at the ends of the cylinder, the length of the airlines as well as compressibility of the line etc, In general, the pressure curve predicted by Eq. (9) shows close agreement with the virtual model. Hence, the predictable solution is employed to analyze the dynamic stiffness of an isolator platform using the air spring with an auxiliary chamber in next section.

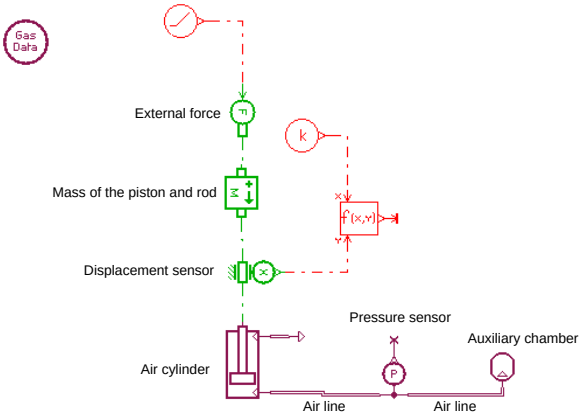

Fig. 3 *Virtual model of the cylinder with auxiliary chamber built by Amesim software for A=0.002m^2, h=150mm, P_o=2.5 bar, V_c= 0.001m^3, 0.01m^3, 0.015m^3 and 0.020m^3*

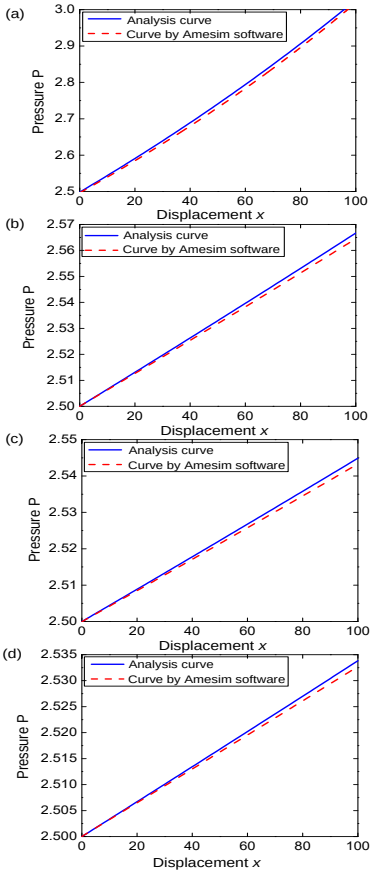

Fig.4 *Predicted pressure with Eq. (6) and pressure obtained from the virtual model for A=0.002m^2, h=150mm, Po=2.5 bar and V_c=1 m^3 in subplot (a); V_c=10 m^3 in subplot (b); V_c=15 m^3 in subplot (c); V_c=20 m^3 in subplot (d); (Detail for the line types is presented in left-corner panel of each figure*)

4. Dynamic stiffness of the isolation platform with auxiliary chamber

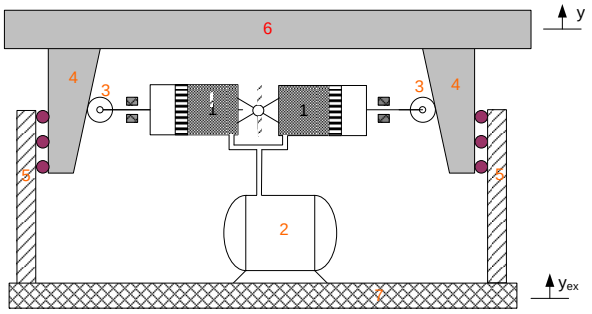

Fig.5 *Isolation platform using the pneumatic cylinder with auxiliary chamber.*

An isolation platform using the air spring with auxiliary chamber (named platform with auxiliary chamber) is introduced in Fig. 5. In this structure, the load plate (6) is supported by two cylinders (1), rollers (3) and the wedges (4). The load plate only moves vertically via the guidable bars (5). During working, the rollers roll without slide on the surface of the wedges.

The vertical resorting force acting on the load plate is expressed as following:

$$F = 2\left(P - P_{atm}\right) A \tan\alpha \qquad (10)$$

where P_{atm} is absolute ambient pressure in Pa, P is the absolute air pressure in the cylinder is given by Eq. (9) and α is the wedge angle.

Eq. (10) is rewritten in dimensionless form as below:

$$\hat{F} = 2\left(\hat{P}_o \left(\frac{1+\hat{V}_{ac}}{1+\hat{V}_{ac} - \hat{y}\tan\alpha} \right)^n - 1 \right) \tan\alpha \qquad (11)$$

in which $\hat{F} = \frac{F}{AP_{atm}}; \hat{P}_o = \frac{P_o}{P_{atm}}; \hat{V}_{ac} = \frac{V_{ac}}{Ah}; \hat{y} = \frac{y}{h}$

in which y is the absolute displacement of the load plate as shown in Fig. 5

By taking differentiation of Eq. (11) with respect to displacement y, the dimensionless vertical stiffness of the isolation platform is explained as below:

$$\hat{K} = 2n\hat{P}_o \frac{\left(1+\hat{V}_{ac}\right)^n}{\left(1+\hat{V}_{ac} - \hat{y}\tan\alpha\right)^{n+1}} \tan^2\alpha \qquad (12)$$

By applying Newton's second law, the dynamic equation of the load plate is expressed as follows:

$$M\ddot{u} + c\dot{u} + F\tan\alpha - Mg = MY_{ex}\cos(\omega t) \qquad (13)$$

in which, M is the weight of the isolated object, c is the coefficient of damping, u is the displacement of the load plate relative the base, F is the vertical restoring force given by Eq. (10), Y_{ex} is the amplitude of the excitation signal from the base as displayed in Fig. 5, α is the inclined angle of the wedge, ω is the excitation frequency, g is the acceleration of gravity.

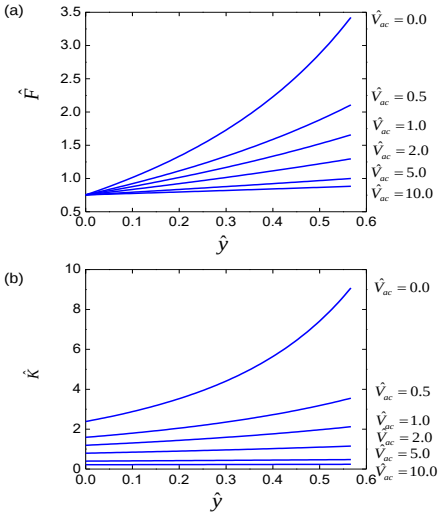

Fig. 6 *The vertical restoring force (a) and dynamic stiffness (b) of the isolation platform under various values of the auxiliary chamber volume.*

Figure. 6 shows us the effects of the volume of the auxiliary chamber on the vertical restoring force and the dynamic stiffness curve of the isolation platform for α=37°. If $\hat{V}_{ac} = 0$ the isolation platform obtains the biggest stiffness and the stiffness of which is a strong nonlinear function with respect to the displacement $\hat{y}$. In addition, it can be noted that there will be a large variation in the stiffness curve for a change in the value of $\hat{V}_{ac}$. As observed, increasing the volume of the auxiliary chamber will produce a low dynamic stiffness and a slow change of stiffness around the static equilibrium position. When the value of $\hat{V}_{ac}$

is larger than 1 ($V_{ac} > Ah$), the variation of the stiffness of the isolation platform versus the dimensionless displacement $\hat{y}$ is small. In the case of $\hat{V}_{ac} > 5$ the stiffness of the LBM is nearly constant in the working region. However, if the volume of the auxiliary chamber is increased remarkably for instance $\hat{V}_{ac} \geq 10$, this causes difficulty in the practical application of the air spring because of the large auxiliary chamber volume. But if the inclined angle of the wedge is designed with a smaller value, the auxiliary chamber is demanded with a smaller value of $\hat{V}_{ac}$ for which the curve of the dynamic stiffness of the LBM is changed slowly around the equilibrium position as shown in Fig. 7(a). In this case, the dimensionless the volume of the auxiliary chamber is set at value of 5, it can be seen that the slope of the stiffness a curve is reduced according to the decrease of the inclined angle.

However, a disadvantage of the growth in the volume of the auxiliary chamber or reduction in the inclined angle is to lower the stiffness of the isolated platform. This can be overcame by increasing the pressure in the cylinder but still to remain the desirable slope of the stiffness curve as denoted in Fig. 7(b).

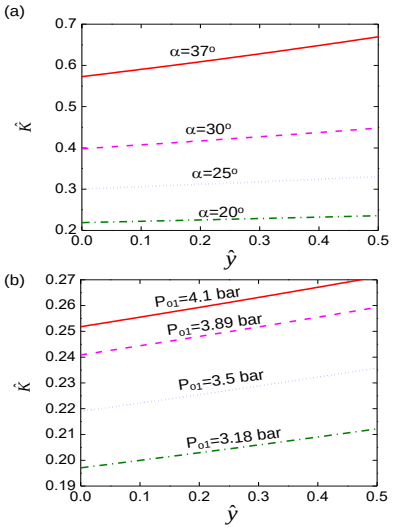

Fig.7 *The stiffness of the platform for (a)* $\hat{V}_{ac} = 5$, P_{o1}*=3.5 bar and various value of* α*;* (b)*for* $\hat{V}_{ac} = 5$, $\alpha = 20^o$ *and various values of* P_{o1}

By using a fourth-order Runge-Kutta algorithm with a fixed time step of 1/100, the numerical integration for Eq. (13) will be realized to obtain the vibration transmissibility curve of the platform. For the compared purpose, the base is excited by the sinusoidal signal ($y_{ex} = Y_{ex}\sin\omega t$) with the amplitude of 10mm and the frequency swept from 0 to 20rad/s. In order to support the load of 150 kg with the static deformation of 40mm, the initial pressures in the cylinder of the platform with and without the auxiliary chamber are set at a value of 2.15 and 1.61 bar, respectively. The vibration transmissibility of the platform with and without an auxiliary chamber is compared as shown in Fig. 8.

Simulation result confirms the benefit of the auxiliary chamber for isolating vibration. In fact, the isolation platform without the auxiliary chamber (exhibited by dashed line) suppresses the vibration that the frequency of which is larger than 15Hz, meanwhile, the frequency region over which the platform with the auxiliary chamber (denoted by the solid line) is effective is greater than 6Hz. In addition, by using the auxiliary chamber, the vibrated attenuation of the platform is better than that of one without the auxiliary chamber.

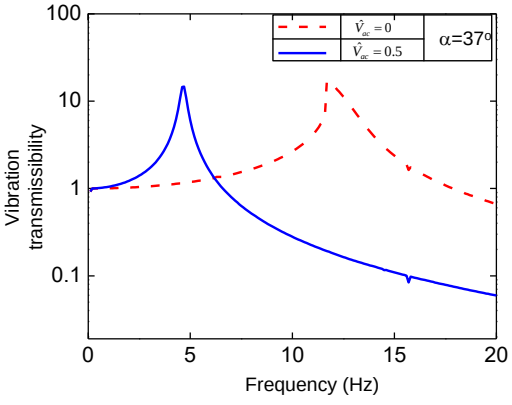

Fig.8 *Comparison of the vibration transmissibility between the platform with and without the auxiliary chamber*

5. CONCLUSIONS

A conceptual design for a vibration isolation platform using the air spring with an auxiliary chamber has been established.

Pneumatic cylinder with auxiliary chamber model has been performed to determine the relationship between the pressure in the cylinder and the volume of the auxiliary chamber corresponding to the displacement of the piston. The virtual simulation results show good agreement with theoretical predictions, in particular, the analysis curve which matches the shape of the curve by Amesim software well. A platform using a pneumatic cylinder with auxiliary chamber has been proposed. The relation between the vertical restoring force and the dynamic stiffness of the isolation platform under various values of the auxiliary chamber volume along with the geometrical parameters of the mechanical structure for the quasi-constant stiffness which is convenient for practical application in vibration isolation.

Acknowledgements

This research is funded by Vietnam National Foundation for Science and Technology Development (NAFOSTED) under grant number 107.04-2016.35.

REFERENCES

[1] Y-S. Wu and C-C. Lan, Linear Variable-Stiffness Mechanisms Based on Preloaded Curved Beams, Journal of Mechanical Design, 136, pp. 1-10, 2014.

[2] B. Chen, Z. Cui and H. Jiang, Producing negative active stiffness in redundantly actuated planar rotational parallel mechanism, Mechanism and Machine Theory, 128, pp.336-348, 2018.

[3] C. Wogerer , G. Nittmann and T. Panner, Isolation of small coil spring, IEEE International Symposium on Assembly and Manufacturing, pp. 130-134, 2007.

[4] S.G. Kelley, Fundamental of mechanical vibrations, McCraw-Hill, 2002.

[5] W. Wu, X. Chen and Y. Shan, Analysis and experiment of a vibration isolator using a novel magnetic spring with negative stiffness, Journal of Sound and Vibration, 333, pp. 2958-2970, 2014.

[6] B. Yan, H. Ma, C. Zhao, C. Wu, K. Wang and P. Wang, A Vari-stiffness nonlinear isolator with magnetic effects: Theoretical modeling and experimental verification, International Journal of mechanical and Sciences, 148, pp.745-775, 2018

[7] A. Carrella, M.J. Brennan, T. P. Waters and K. Shin, On the design of a high-static–low-dynamic stiffness isolator using linear mechanical springs and magnets, Journal of Sound and vibration, 315, pp. 712-720, 2008.

[8] Y. Zheng, Q. Li, B. Yan, Y. Lu and X. Zheng, A stewart isolator with high-static–low-dynamic stiffness struts based on negative stiffness magnetic springs, Journal of Sound and vibration, 422, pp. 390-408, 2018.

[9] M.W. Holtz and J.L.V. Niekerk, Modeling and design of a novel air-spring for a suspension seat, Journal of Sound and vibration, 329, pp. 4354-4366, 2010.

[10] I. Maciejewski, L. Meyer and T. Krzyzybski, The vibration damping effectiveness of an active seat suspension system and its robustness to varying mass loading, Journal of Sound and vibration, 329, pp. 3898-3914, 2010.

[11] I. Maciejewski, Control system design of active seat suspension, Journal of Sound and vibration, 331, pp. 1291-1309, 2012.

[12] I. Maciejewski, S. Glowinski and T. Krzyzybski, Active control of a seat suspension with the system adaptation to varying load mass, Mechatronics, 24, pp. 1242-1253, 2014.

[13] S. Oman, M. Fajdiga and M. Nagode, Estimation of air-spring life based on accelerated experiments, Material and Design, 31, pp. 3859-3868, 2010.

[14] M.M. Moheyeldein, A.M. Abd-El-Tawwab, K.A. Abd El-gwwad band M.M.M Salem, An analystical study of the performance indices of air spring suspensions over the

passive suspension, Beni-Suef University Journal of Basic and Applied Sciences, 7, pp. 525-534, 2018.
[15] C.M. Lee, A.H. Bogatchenkov, V.N. Goverdovskiy, Y.V. Shynkarenko and A. I. Temnikov, Position control of seat suspension with minimum stiffness, Journal of Sound and Vibration, 292, pp. 435-442, 2006.
[16] R.G. Todkar, Design, development and testing of an air damper to control the resonant response of a SDOF quarter-car suspension system, Modern Mechanical Engineering, 1, pp. 84-92, 2011.
[17] R.G. Todkar and S. G. Joshi, The effect of mass ratio and air damper characteristics on the resonant response of an air damper dynamic vibration absorber, 1, pp. 93-103, 2011.

Corresponding author:
Le Thanh Danh
Ton Duc Thang University
Email: lethanhdanh@tdtu.edu.vn